

# LES-based generation of time sequential data of instantaneous urban wind in typhoon -comparison with observational data

**Masaharu Kawaguchi**

Department of Architecture and Building Engineering  
Tokyo Institute of Technology  
Ookayama 2-12-1, Meguro, Tokyo, 152-8550, Japan  
kawaguchi.m.ag@m.titech.ac.jp

**Tetsuro Tamura**

Department of Architecture and Building Engineering  
Tokyo Institute of Technology  
Ookayama 2-12-1, Meguro, Tokyo, 152-8550, Japan  
tamura.t.ab@m.titech.ac.jp

## ABSTRACT

In this paper, LES of urban area was performed using inflow turbulence with meteorological disturbance of strong typhoon Hagibis (2019) and the simulated turbulent characteristics are compared with the field measurement data. The method is further applied to the analysis of the wind pressure on a building in a densely built-up area.

## BACKGROUND

Strong tropical cyclones, such as typhoons and hurricanes, strike cities in the temperate zone more frequently in recent years and raised great concerns for urban environment safety. It is important to accurately simulate velocity variability in densely built-up areas and evaluate the peak value of wind pressure acting on buildings in such extreme weather events. For assessing wind resistance design of buildings, more realistic replication of actual atmospheric conditions including detailed flow structures of severe storms is anticipated. Previously, Kawaguchi and Tamura et al. (2021) performed a large eddy simulation (LES) of the urban flow field in the significant Typhoon Jebi (2018), and the influence of the meteorological field on the formation of near-ground gusts was analyzed. This paper aims to compare turbulence characteristics reproduced in the LES analysis using inflow with meteorological disturbance to the surface observational data in the case of the strong Typhoon Hagibis (2019) and apply further to evaluate the wind load on an actual building in the urban area Shibuya.

## METHOD

To perform a LES of an urban area using the inflow turbulence based on the meteorological model simulation, three different simulations were conducted in series as shown Figure 1.

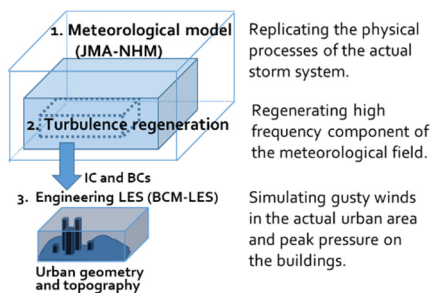


Figure 1. Framework of the hybrid meteorological/engineering LES method.

Firstly, a meteorological model simulation was performed to replicate the detailed structure and movement of the typhoon. Secondly, high frequency components attenuated in the meteorological field were regenerated using the meteorological model/engineering LES hybrid method (Kawaguchi, Tamura et al., 2019). Finally, the LES of the target urban area was carried out by an LES with the turbulent inflow obtained in the previous simulations.

Typhoons Hagibis (2019) was simulated using Japan Meteorological Agency Nonhydrostatic Model (JMA-NHM; Saito et al., 2006). Triply nested domains with resolutions of 1 km, 250 m, 50 m were employed as shown Figure 2. Grid resolution and other configurations of domains are described in Table 1. The initial time of the outermost domain was set to 15:00 on October 12, 2012, in Japan Standard Time (JST). Initial and boundary conditions of the outermost domain were provided with the JMA mesoscale analysis. For cloud microphysics, a bulk-type scheme that predicts the mixing ratios of six water species was utilized. In all three domains, subgrid turbulent mixing is treated using a 1.5-order turbulent kinetic energy closure scheme.

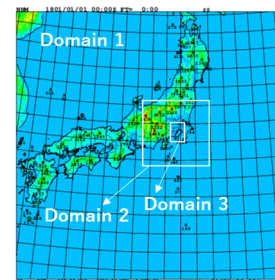


Figure 2. Calculation domains.

Table 1. Domain configuration of JMA-NHM.

Domain	Dimensions [grid points]	Horizontal grid spacing [m]	Time step [s]
D1	1601*1601*92	1000	3
D2	1601*1401*100	250	1
D3	1101*1781*100	50	0.25

In order to enhance the fine turbulent flow structures attenuated in the meteorological model, two sets of LES for turbulence regeneration were executed at 25-m resolution

focusing for each urban area of the subsequent simulation. The dimension of the calculation domains is 12-km (E–S)\*7-km (N–S)\*2.7-km (vertical). Numerical schemes and other calculation conditions were listed in Table 2.

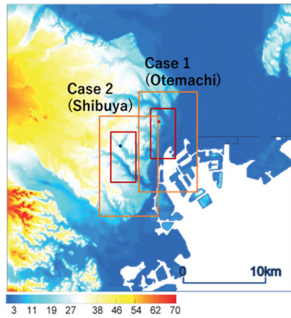


Figure 3. Domains of the turbulence regeneration calculation (Orange boxes) The red boxes correspond to the domains of subsequent LES of the urban areas.

Table 2. Calculation conditions for turbulence regeneration.

Domain dimensions [grid points]	480 (N-S) *280 (E-W) *60 (vertical)
Horizontal grid spacing [m]	25
Vertical grid spacing [m]	18.1–70.5
Calculation period	20:48:00 – 21:00:00 (JST)
Time step [s]	0.02s
Time integration	2 <sup>nd</sup> order Adams–Bashforth (for advection term) 1 <sup>st</sup> order Euler explicit (for other terms)
Spatial discretization	4 <sup>th</sup> order central difference (for velocity) 2 <sup>nd</sup> order central difference (for equivalent potential temperature)
Pressure solver	SOR

The LES of the actual urban areas during the closest approach of Typhoon Hagibis was performed for two districts in Tokyo: Otemachi district, where the observation site of JMA Tokyo Regional Headquarters (Tokyo RHQ) is located, and Shibuya district, which is a densely built-up area.

For each case, the calculation domain was set to have a dimension of 6 km\*3 km\*1.5 km, and the minimum resolution at 1.5 m. For Case 2, the central part of Shibuya district (1.9km\*1.9km\*0.95km) was further one-way nested to a domain with 93-cm resolution grids and separately simulated for evaluation of wind load on the target building. Figure 4 shows the calculation domains of Case 1 (Otemachi), Case 2 (Shibuya), and Case 3 (Shibuya, nested). The number of computational grids were 0.72 billion, 0.59 billion, and 0.35 billion, respectively. Timestep increment was set to 0.005 s. The simulation was performed for the period between 20: 48 and 21:00 (2 min for field initialization and 10 min for analysis).

The realistic turbulent flow in the typhoon obtained in the previous steps was used for the initial field and the inflow data at the south, east, and west boundaries. CUBE developed by RIKEN R-CCS was used for the numerical solver. The solver incorporates a multi-block hierarchical Cartesian grid system

and immersed boundary method to perform hyper large parallel computation in an optimum load balance.

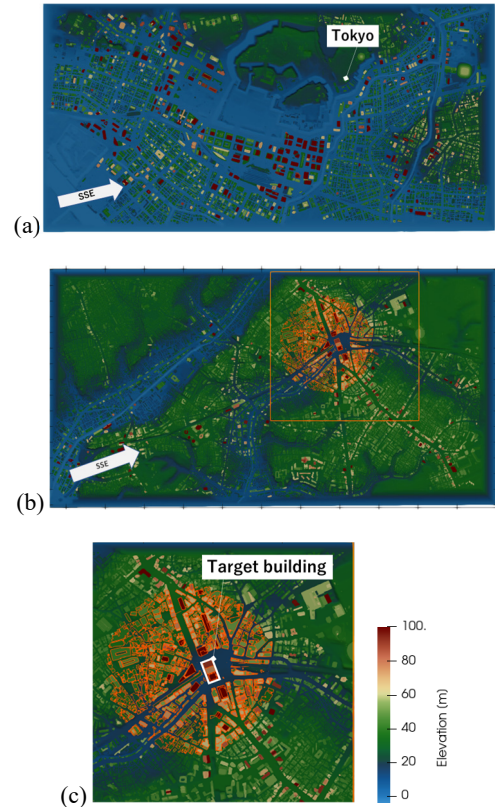


Figure 4. Surface models for LES of urban area. (a) Case 1, Otemachi (White dot indicates the observation site). (b) Case 2, Shibuya. (c) Case 3, Shibuya, detailed analysis.

## GENERATION OF THE METEOROLOGICAL DISTURBANCE INFLOW

Figure 5 shows the actual and simulated typhoon tracks and central pressure. Simulated typhoon roughly followed the actual track and made the closest approach to the target area about the same time, around 21:00. Although the track had been improved from the preliminary cases where the initial time was set earlier, it shifted about 40-50 km to the northwest. The simulated central pressure was slightly lower than the actual case during the typhoon's closest approach to the target area. In order to improve the reproduction of track and intensity and consider uncertainty of the event, the use of ensemble analysis may be effective.

Figure 6 shows the velocity fields at different altitudes at the closest approach time. The meteorological model simulation successfully reproduced cumulonimbus and finer wind speed fluctuations based on longitudinal vortices in the typhoon boundary layer. Bands of high and low wind speeds were apparently aligned in the wind direction at intervals of several kilometers.

Using the method of Kawaguchi and Tamura et al. (2019), high frequency component was regenerated to the meteorological field. The visualization of the horizontal cross-section and the time history in Figure 7 shows that fine turbulent structures were generated based on the meteorological field through the turbulence energy cascade.

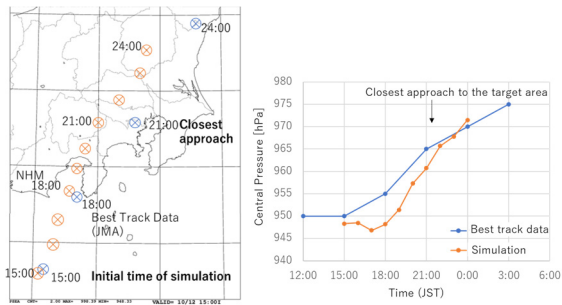


Figure 5. Actual and simulated typhoon tracks and central pressure of Typhoon Hagibis (2019)

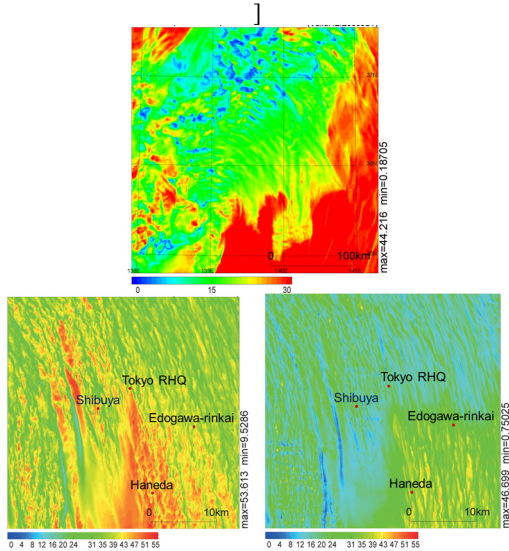


Figure 6. Velocity fields of Typhoon Hagibis (2019) simulated with JMA-NHM. Result of Domain 1 at  $z=85$  m above ground level (AGL) (top). Result of Domain 3, at  $z=146$  m AGL (lower left) and 30 m AGL (lower right).

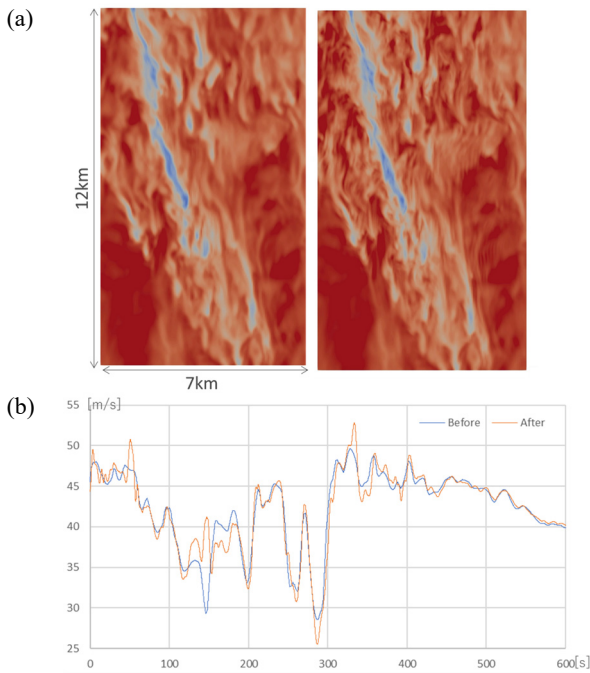


Figure 7. Turbulence regeneration to the meteorological field. (a) Velocity field of Case 2 at  $z=300$  m AGL before (left) and after (right) the turbulence regeneration. (b) Time series of wind speed at  $z=430$  m.

### COMPARISON OF THE NEAR-GROUND TURBULENCE WITH THE OBSERVATIONAL DATA

Near-ground turbulence in Case 1 was compared with observational data at Tokyo RHQ during the closest approach of Typhoon Hagibis. The location of the observation site is indicated in Figures 4(a).

Figure 8 shows instantaneous velocity fields at 300m above sea level (ASL), 200 m ASL, and 56 m ASL. (The elevation at Tokyo RHQ is about 20 m.) Turbulent structures shown in Figure 7 intruded over the urban area. Wake regions of high-rise buildings is extended downward to a considerable extent, making bands of wind speed fluctuation. Local variation of the wind direction is evident near the ground.

Figure 9 shows the time history of the simulated wind speed and the spectra of horizontal wind speed at Tokyo RHQ, at the altitudes  $z = 300$  m and 40 m. The waveform showed very fine and acute velocity fluctuations. The spectra reveal that reproduced turbulence was in accordance with Kolmogorov's -5/3 power law up to approximately 0.5 Hz at an altitude of 300 m, and to frequencies above 1 Hz at an altitude of 40 m. The low-frequency side of the spectrum maintained a large amount of energy, suggesting that a broadband turbulent inflow wind with meteorological disturbances was successfully obtained.

The wind profile at Tokyo RHQ and visualizations of instantaneous velocity field in the vertical cross-sections are shown in Figure 10. The simulated wind profile was a power-law type, although it was observed that longitudinal vortices locally and continuously transferred high winds to near-ground region.

JMA now publicly releases their observational data resampled in 10-s interval. In Figure 11, the simulated wind speeds were compared with the observational data at Tokyo RHQ. The time series of 3-s maximum and minimum gust speeds during 10 s of evaluation time and 10-s mean wind speed are shown along with the time history of 10-s mean wind direction. From the velocity waveforms of the observation, considerable variability of turbulent intensity or gust ratio in time exists and the influence in actual field. Especially, gust ratio was significantly increased around velocity maxima. The simulated time series also reproduced variability of turbulent intensity, although it has somewhat different waveform and peak pattern from those of observation. Fluctuation of wind direction was evident in both of the simulation in the present method and the observation. The waveform of the simulation contains many cycles of fluctuation in the range of about 45 to 90 degrees. Fluctuation amplitude of the observation was even larger.

Table 3 shows statistics of wind speed simulated and measured at Tokyo RHQ. The simulated mean wind speed was about 5 m/s higher than the observation, while the estimated maximum wind gust was not as high as the actual case.

The result show that the present method at current stage cannot always predict exact turbulence condition at a particular location and time during the actual extreme weather event. Yet, the near-ground flow field was successfully analyzed with appropriate inflow turbulence that reflects characteristics of meteorological field strong typhoon. Differences are most likely to be attributed to the reproducibility of the event such as intensity and track of the typhoon. Previous research reported the difference of wind profiles (Franklin, 2003; Kepert and Wang, 2001) and the near-surface coherent structures (Ito et al., 2017) depending on the distance from the tropical cyclone core. Uncertainty of the turbulent phenomena and structure of meteorological field has also influence on the result.

The improvement of qualitative reproducibility of the phenomena and quantitative accuracy by utilizing the ensemble analysis data will be the subject of future research.

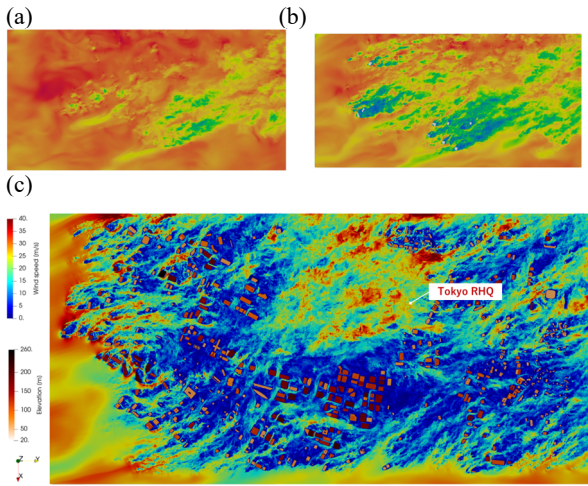


Figure 8. Instantaneous wind speed in the urban area of Otemachi. (a) 300 m above sea level (ASL). (b) 200 m ASL. (c) 56 m ASL.

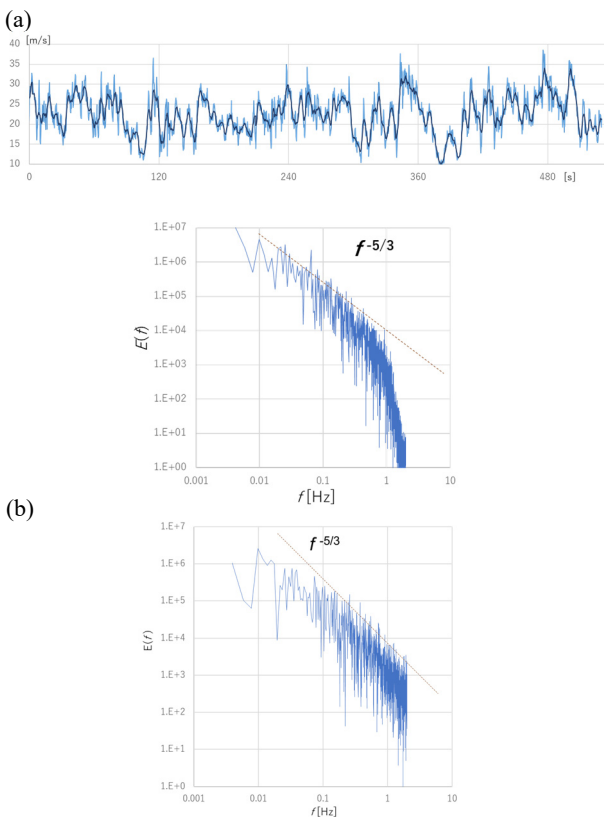


Figure 9. Wind speed simulated at the observation site at  $z=40$  m above ground level (AGL). (a) Time series of 3-s mean wind speed (dark blue) and instantaneous value (light blue). (b) Spectra of wind speed fluctuation at 300 m AGL (top) and 40m AGL (bottom).

Table 3. Comparison of statistics of wind speed.

	Mean	Max 3-s gust	Turbulence intensity (10-s mean wind)
LES (40m AGL)	22.4	34.0	16.4
Obs. (35.3m AGL)	17.8	41.5	26.9

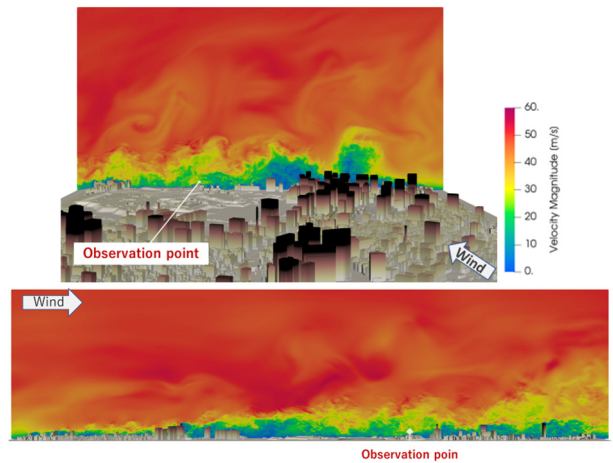
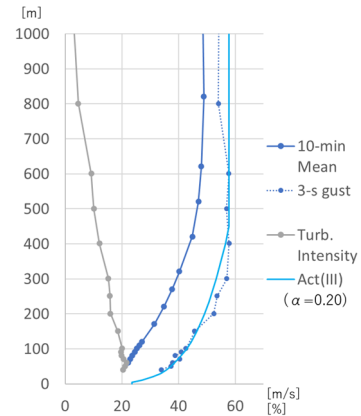


Figure 10. Vertical profile at the observation point and visualizations of instantaneous wind speed in the cross-sections approximately perpendicular and parallel to wind direction.



Figure 11. Time series of horizontal wind speed and direction of Case 1. Simulation result (top), observational data (bottom). Orange and blue lines show the 3-s maximum and minimum in 10 s of evaluation time. Dark gray lines 10-s averaged wind direction.

### OCCURRENCE OF STRONG GUSTS IN THE HIGHLY BUILT-UP URBAN AREA

In Case 2, the pattern of strong gusts occurrence was analyzed in a highly built-up urban area Shibuya. Figure 12 shows the distribution of mean and maximum instantaneous wind speeds within the urban area at 100 m ASL, 50 m ASL and 25m ASL. (The elevation at the target building is approximately 15 m); a similar tendency to the results in Osaka during Typhoon Jebi (2018) was observed.

At 100 m ASL, numerous trajectories of high-speed gusts were observed running downstream several hundred meters with a narrow width about 100 m. Many of the them were straight, slightly deviating from the direction of the mean flow. Larger-scale variation due to the flow structures of the meteorological field seems to be superimposed.

At 50 m ASL, streaky strong wind patterns in more random directions were observed and high wind were evident in open areas and near the high-rise buildings.

At 25 m ASL, strong gusts were similarly prominent around high-rise buildings, but was further transported near the ground along the downstream streets, including areas with relatively small mean velocities.

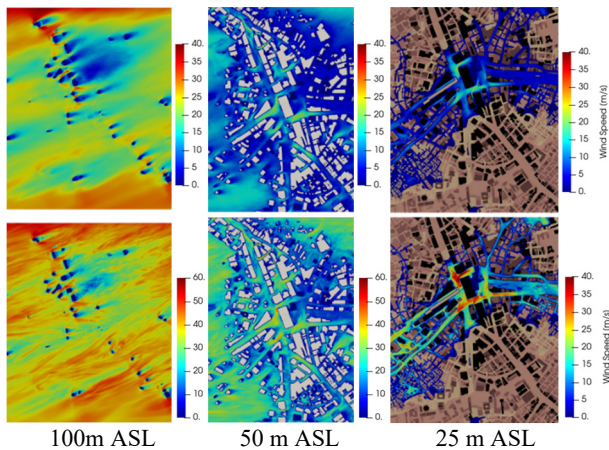


Figure 12. Distribution map of mean wind speed (top row) and 3-s maximum wind speed (bottom row) in the central area of Shibuya in Case 2

### ESTIMATION OF WIND LOAD ON THE BUILDING

In Case 3, the wind pressure acting on the target building was estimated by the analysis of downtown of Shibuya district in the nested domain from Case 2 with 93-cm grid resolution.

Figure 13(a) shows the spatial distribution of wind pressure coefficients on the target building in Figure 4(c). The averaging time for peak wind pressure is 0.3 s. As the majority of the building is situated in the wake region of the adjacent upstream high-rise building, large positive pressure was exerted only on the upper part of the high-rise towers. Negative peak wind pressure was found at the front edge of the side wall of high-rise building near where the flow over the upstream building acted.

The time history of the pressure coefficient at point P, where the maximum negative pressure was experienced, is shown in Figure 13(b). The result with 93-cm grid (about 1/75th of the building width) reproduced sharp pressure drop in time history. The minimum value reached -2.7 at 411 s. The same result obtained in Case 2 with a resolution of 1.5 m (approximately 1/47th of the building width) is presented in the same figure. Analysis yielded similar fluctuation trends, but with much smaller amplitudes. Vortex generation is not captured clearly, due to use of immersed boundary method in insufficient resolution.

The time history shows that significantly strong negative pressure was frequently occurred during a couple of minutes before and after the minimum wind pressure. The time history of wind speed at upstream from the target building shown in Figure 13(c) reveals that it was coincided with the increase of wind speed. The instantaneous wind speed in the cross-wise vertical section at 411 s shown in Figure 13(d) reveals that it was caused by the flow structure of the meteorological field structure which locally lowered at the location of the building.

Figure 13(e) shows the 3D iso-surfaces of pressure coefficient -1, -2, -3 around the target building at 411 s. Strong inverted conical vortex developed at about the height where the shear layer of the upstream building roof hit and it was stretched in the wind shear in vertical direction.

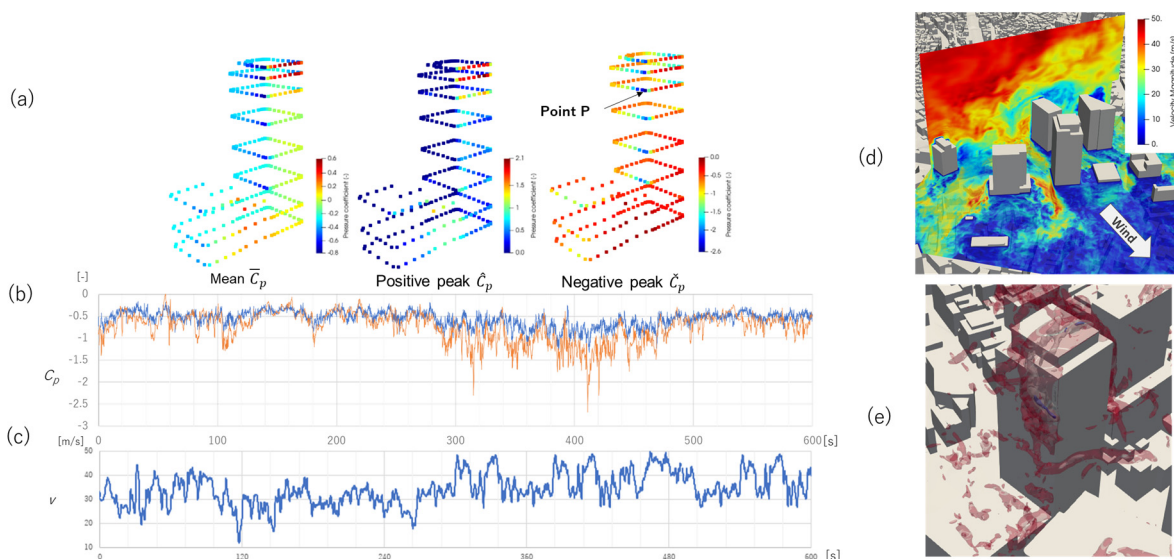


Figure 13. Evaluation of wind loading. (a) Spatial distribution of pressure coefficient on the target building in Case 3. (b) Time series of the pressure coefficient at Point P obtained in Case 2 at 1.5m resolution (blue) and in Case 3 at 93-cm resolution (orange). (c) The time history of wind speed at 300 m upstream from the target building. (d) Instantaneous wind speed in the cross-wise vertical section at 411 s (e) 3D iso-surfaces of pressure coefficient -1, -2, -3 around the target building at 411 s

## CONCLUSIONS

In this study, we performed LES of actual urban areas in Tokyo, Japan, using the meteorological model/engineering LES method to reproduce the event of approach of strong typhoon Hagibis (2019) and compared the simulation result to the ground observation of wind speed and direction.

In the innermost domain of the meteorological model simulation at a resolution of 50 m, longitudinal vortex in the typhoon boundary layer and fine wind speed fluctuation were successfully generated. However, the track shifted 40-50 km to the northwest, and the central pressure was slightly ( $\sim 5$ hPa) lower than the actual case. This result presented the difficulty in replicating actual weather events with sufficient accuracy necessary for a city-scale simulation by deterministic analysis.

LES analysis of an actual urban area (Otemachi, 6km\* 3km) was performed at a resolution of 1.5 m with inflow turbulence replicating Typhoon Hagibis. The spectral analysis confirmed the generation of broadband turbulence, following Kolmogorov's -5/3 power law, up to frequency higher than 1 Hz at 40 m height. The low-frequency side of the spectrum maintained a large amount of energy, which is expected to be caused by meteorological disturbances.

Comparison between the time histories of velocity of LES analysis and observed turbulent wind in Typhoon Hagibis indicated some qualitative similarities, such as considerable variations of turbulent intensity and wind direction within 10 min of evaluation time, although qualitative reproducibility of the meteorological disturbance and quantitative estimation of turbulence statistics were not satisfactory yet.

The discrepancy between the numerical simulation and the actual meteorological field can be primarily caused by the difference of wind profile and coherent longitudinal vortex structure, which varies depending on the distance from the typhoon core. The track and intensity of track can be affected significantly by the uncertainty in the meteorological model simulation of initial and boundary conditions. Stochastic nature of turbulence and flow instability may also have some influence.

Further improvement will be sought through LES of urban areas coupled with ensemble analysis that reproduces the uncertainties of the meteorological simulation.

Subsequently, LES of the highly built-up urban area, Shibuya was performed at the 1.5-m resolution, and the patterns of strong gusts occurrence at different altitudes were presented.

Similarities to the prior study in the mid-rise urban area were observed.

Finally, the unsteady pressure acting on a high-rise building was analyzed by LES in a nested domain from the above analysis. Prediction of sharp negative peak pressure was significantly improved at the 93-cm resolution (about 1/75th of the building width), in comparison with the result at the 1.5-m resolution (about 1/47th of the building width).

## ACKNOWLEDGMENTS

This work used computational resources of the supercomputer Fugaku provided by RIKEN through the HPCI System Research Projects (Project ID: hp210158, hp210262).

## REFERENCES

- Franklin, J., Black, M., Valde, K., 2003, "GPS Dropwindsonde Wind Profiles in Hurricanes and Their Operational Implications," *Weather and Forecasting*, Vol.13, 32-44.
- Ito, J., Oizumi, T., and Niino, H., 2017, "Near-surface coherent structures explored by large eddy simulation of entire tropical cyclones," *Scientific reports*, Vol.7(1), 1-10.
- Kawaguchi, M., Tamura, T., and Kawai, H., 2019, "Analysis of tornado and near-ground turbulence using a hybrid meteorological model/engineering LES method," *International Journal of Heat and Fluid Flow*, Vol. 80, 108464.
- Kawaguchi, M., Tamura, T., and Mashiko, W., 2021, "Application of hybrid meteorological model/engineering LES analysis to very strong Typhoon Jebi 2018," *Proceedings, the 13th International ERCOFTAC symposium on engineering, turbulence, modelling and measurement*.
- Kepert, J., Wang, Y., 2001, "The dynamics of boundary layer jets within the tropical cyclone core. Part II: Nonlinear enhancement," Vol.58(17), 2485-2501.
- Saito, K., Fujita, T., Yamada, Y., Ishida, J. I., Kumagai, Y., Aranami, K., Ohmori, S., Nagasawa, R., and Yamazaki, Y., 2006, "The operational JMA nonhydrostatic mesoscale model," *Monthly Weather Review*, Vol. 134(4), 1266-1298.